

CBPF-NF-039/83

SQUARE-LATTICE RANDOM POTTS MODEL: CRITICALITY
AND PITCHFORK BIFURCATION

by

Uriel M.S. COSTA* and Constantino TSALLIS

Centro Brasileiro de Pesquisas Físicas - CNPq/CBPF
Rua Dr. Xavier Sigaud, 150
22290 - Rio de Janeiro, RJ - Brasil

*On leave of absence from Departamento de Física,
Universidade Federal de Alagoas,
57000 - Maceió - Brazil

SQUARE-LATTICE RANDOM POTTS MODEL: CRITICALITY
AND PITCHFORK BIFURCATION

Uriel M.S. COSTA*

Constantino TSALLIS

Centro Brasileiro de Pesquisas Físicas/CNPq
Rua Xavier Sigaud, 150
22290 - Rio de Janeiro, RJ - BRAZIL

*On leave of absence from Departamento de Física,
Universidade Federal de Alagoas,
57000 - Maceió - BRAZIL

ABSTRACT

Within a real space renormalization group framework based on self-dual clusters, we discuss the criticality of the quenched bond-mixed q -state Potts ferromagnet on square lattice. On qualitative grounds we exhibit that the crossover from the pure fixed point to the random one occurs, while q increases, through a pitchfork bifurcation; the relationship with Harris criterion is analyzed. On quantitative grounds we present high precision numerical values for the critical temperatures corresponding to various concentrations of the coupling constants J_1 and J_2 , and various ratios J_1/J_2 . The pure, random and crossover critical exponents are discussed as well.

I - INTRODUCTION

During the last few years, considerable theoretical effort has been dedicated to random magnetism, concerning in particular models such as the Ising, Heisenberg and Potts ones (for an excellent review of the latter see Ref. [1]). Because of its richness the Potts model has recently received special attention, in particular its quenched bond-random version, which has been studied within effective-field [2,3], duality-based [4-8] and real space renormalization group (RG) [9,10] approaches. One of the interesting features of the q -state Potts ferromagnet is related to the Harris criterion [10-14], initially stated for the Ising model ($q = 2$) but presumably correct for any value of q (at least as long as second order phase transitions are concerned). According to this criterion, if the specific heat critical exponent α of the pure model is negative (positive), the criticality—to be more precise the set of critical exponents—of the diluted or more generally the random model is (is not) that of the pure model; in the RG language, a new fixed point, namely the random one, is expected to appear for $\alpha > 0$. Furthermore if we assume hyperscaling (i.e., $2 - \alpha = d\nu$, where d is the dimensionality of the system, and ν is the correlation length critical exponent), the frontier between the pure and random critical regimes (i.e. $\alpha = 0$) should correspond to $\nu = 2/d$; for planar Potts ferromagnetics, this implies $\nu = 1$ hence $q = 2$. However this fact is of course associated with the thermodynamical limit (macroscopic system), and in principle there is no reason for remaining unchanged within a finite cluster RG ap-

proach, which frequently is related to hierarchical-like lattices (and not to Bravais lattices). This problem is analyzed in the present paper where, by using self-dual clusters and following along the lines of Ref. [15] (RG treatment of the bond-mixed Ising ferromagnet) we calculate the critical temperature T_c as well as the critical exponents ν and ϕ (crossover exponent) for the square-lattice Potts ferromagnet.

The present work is organized as follows: in Sections II and III we introduce the model and the RG framework respectively, and, in Section IV, we present the results (which are of considerable precision ones for the critical temperatures but only approximate for the critical exponents); finally we conclude in Section V.

II - MODEL

Let us consider the following Hamiltonian

$$\mathcal{H} = -q \sum_{\langle i,j \rangle} J_{ij} \delta_{\sigma_i, \sigma_j} \quad (\sigma_i = 1, 2, \dots, q, \forall i) \quad (1)$$

where the sum runs over all pairs of first-neighboring sites on a square lattice, and J_{ij} is a random variable whose probability law is given by

$$P(J_{ij}) = (1-p) \delta(J_{ij} - J_1) + p \delta(J_{ij} - J_2) \quad (2)$$

with $J_1 \geq 0$, $J_2 > 0$ and $0 \leq p \leq 1$. We notice that the pure Potts

ferromagnet can be recovered with $p = 0$, $\forall J_2$, or $p = 1$, $\forall J_1$, or even $J_1 = J_2$, $\forall p$; the case $\gamma \equiv J_1/J_2 = 0$ corresponds to the diluted model.

The complete critical frontier (in the $p - k_B T/J_2 - \gamma$ space, for example) of this model is still unknown; however a few partial exact results are already available, namely (see, for example, Ref. [5] and references therein):

i) for the pure Potts model (e.g. $p = 1$, $\forall J_1$):

$$e^{qJ_2/k_B T_c} = \sqrt{q} + 1; \quad (3)$$

ii) for the bond percolation model ($\gamma = 0$ and $T = 0$):

$$p_c = 1/2 \quad , \quad \forall q \quad ; \quad (4)$$

iii) for the equal-concentration model ($p = 1/2$) [5,10] :

$$e^{qJ_2/k_B T_c} = \frac{e^{qJ_1/k_B T_c} + q - 1}{e^{qJ_1/k_B T_c} - 1} \quad ; \quad (5)$$

iv) for the $q \rightarrow 1$ limit (isomorphic to bond percolation [16]):

$$(1 - p)(1 - e^{-J_1/k_B T_c}) + p(1 - e^{-J_2/k_B T_c}) = 1/2; \quad (6)$$

v) for the bond-diluted almost pure Potts limit ($\gamma = 0$ and $p \rightarrow 1$):

$$\left. \frac{1}{T_c(1)} \frac{dT_c(p)}{dp} \right|_{p=1} = \frac{2\sqrt{q}}{(1 + \sqrt{q}) \ln(1 + \sqrt{q})} \quad (7)$$

vi) for the bond-diluted almost bond percolation limit ($\gamma = 0$ and $T \rightarrow 0$):

$$\left. \frac{de^{-qJ_2/k_B T_c(p)}}{dp} \right|_{p=p_c} = \frac{2 \ln q}{q-1} \quad (8)$$

For arbitrary p, J_1 and J_2 , quite precise approximate numerical values for T_c can be obtained from the proposal [5]

$$(1-p) \frac{\ln [1 + (q-1)e^{-qJ_1/k_B T_c}]}{\ln q} + p \frac{\ln [1 + (q-1)e^{-J_2/k_B T_c}]}{\ln q} = \frac{1}{2} \quad (9)$$

which satisfies Eqs. (3) - (6) and (8), but slightly fails with regard to Eq. (7) if $q \neq 1$.

With respect to the critical exponent ν associated with the bond-random Potts ferromagnet with $q \leq 4$ (continuous phase transition [1,17]), it is either well established or commonly believed [11,14] that:

i) for $0 \leq q \leq 2$ and $T > 0$,

$$\alpha(\text{random}) \equiv \alpha_r = \alpha(\text{pure Potts}) \equiv \alpha_t \quad (10)$$

hence, through $2 - \alpha = 2\nu$,

$$\nu(\text{random}) \equiv \nu_r = \nu(\text{pure Potts}) \equiv \nu_t \quad (10')$$

where [18]

$$\nu_t = \frac{2}{3} \left\{ 2 + \frac{\pi}{\arccos(\frac{1}{2}\sqrt{q}) - \pi} \right\}^{-1} ; \quad (11)$$

ii) for $2 < q \leq 4$ and $T > 0$,

$$\alpha_r < \alpha_t \quad (12)$$

hence

$$v_r > v_t \quad (12')$$

where v_t is still given [18] by Eq. (11);

iii) for $T = 0$, $\forall q$

$$v_r = v(\text{percolation}) \equiv v_p = 4/3 \quad (13)$$

as can be recovered from Eq. (11) in the limit $q \rightarrow 1$ [16].

Finally the crossover critical exponent ϕ_p associated with the percolation point satisfies [19]

$$\phi_p = 1 \quad \forall q \quad (14)$$

In the next Section we introduce a RG which enables the calculation of both T_c and v , as well as it gives an insight on how the crossover from the pure to the random behavior occurs.

III - RENORMALIZATION GROUP

Before constructing the RG recursive relations, let us associate, with every bond characterized by an arbitrary coupling constant J_k , a convenient variable (hereafter referred to as thermal transmissivity; see Ref. [20]; also Ref. [5] and references therein) defined as follows:

$$t_k \equiv \frac{1 - e^{-qJ_k/k_B T}}{1 + (q-1)e^{-qJ_k/k_B T}} \quad (15)$$

The transmissivity $t_s(t_p)$ of a series (parallel) array of two bonds with transmissivities t_1 and t_2 , is given ^[21] by

$$t_s = t_1 t_2 \quad (\text{series}) \quad (16)$$

$$t_p^D = t_1^D t_2^D \quad (\text{parallel}) \quad (17)$$

where

$$t_k^D \equiv \frac{1 - t_k}{1 + (q-1)t_k} \quad (k = 1, 2, p) \quad (18)$$

(D stands for dual). Any two-terminal array (or graph) reducible in series/parallel sequences can be solved by using algorithms (16) and (17). More complex two-terminal arrays (e.g. those appearing in Figs. 1.b and 1.c) can be solved through the Break-collapse Method (BCM) ^[21].

Let us now introduce a second convenient variable ^[5] s through

$$s(t) \equiv \frac{\ln[1 + (q-1)t]}{\ln q} \quad (19)$$

which satisfies an interesting property, namely

$$s^D(t) \equiv s(t^D) = 1 - s(t) \quad (20)$$

Because of this property, the variable s has proved ^[4-6,8,15,22] to be extremely performant for the calculation of critical temperatures; we shall use it later on to construct the present RG.

Within our RG (which follows along the lines of Ref. [15]) we shall renormalize the $b = 2$ graph of Fig. 1(b) into the graph of Fig. 1(a) (b is the linear scaling factor; it also characterizes the size of the cluster, as illustrated in Fig. 1). The next-order RG we shall consider consists in renormalizing the $b = 3$ graph of Fig. 1(c) into the graph of Fig. 1(a). This family of graphs preserves a very important topological invariance of the square lattice, namely self-duality, and has already proved to be extremely performant for the treatment of random-resistor [23-26], bond-percolation [27,28], Ising [15,29-31], Heisenberg [32] and Potts [9,21,33] problems. Such choice of clusters systematically provides, among others, the exact critical points corresponding to all the above models in square lattice; it can of course be alternatively looked as referring to hierarchical lattices (see Ref. [32] and references therein).

Let us now proceed to the establishment of the $b = 2$ RG recursive relations. The distribution law (2) can be rewritten as follows:

$$P(t) = (1-p)\delta(t-t_1) + p\delta(t-t_2) \quad (21)$$

where definition (15) has been used. We associate now this distribution with every bond of the $b = 2$ Wheatstone-bridge graph (Fig. 1(b)) and obtain a new and more complex distribution law P_G given by

$$P_G(t) = \sum_{r_1=t_1, t_2} \sum_{r_2=t_1, t_2} \cdots \sum_{r_5=t_1, t_2} (1-p)^{n_1} p^{5-n_1} \delta[t-t_G(r_1, r_2, \dots, r_5)] \quad (22)$$

where n_1 is the number of bonds with transmissivity t_1 appearing in the particular configuration (among 2^5 possible ones) of $\{r_1\}$ we are considering; $t_G(r_1, r_2, \dots, r_5)$ has been calculated through the BCM^[21] (see Ref. [9] for a more standard calculation) and is given by

$$t_G(r_1, r_2, \dots, r_5) = \frac{r_1 r_2^{+r_3 r_4^{+r_1 r_4 r_5^{+r_2 r_3 r_5^{+(q-2)(r_1 r_2 r_3 r_4^{+r_1 r_2 r_3 r_5^{+r_1 r_2 r_4 r_5^{+r_1 r_3 r_4 r_5^{+r_2 r_3 r_4 r_5}}}}}}}}}{1+(q-1)(r_1 r_3 r_5^{+r_2 r_4 r_5^{+r_1 r_2 r_3 r_4}} + (q-2)(q-3)r_1 r_2 r_3 r_4 r_5 + (q-1)(q-2)r_1 r_2 r_3 r_4 r_5} \quad (23)$$

We can verify that the sum of the coefficients of the numerator equals the sum of the coefficients of the denominator and both equal^[21,34] q^κ , where $\kappa \equiv$ cyclomatic number \equiv (number of bonds) - (number of sites) + 1; for the present graph $\kappa = 2$.

Equation (22) can be rewritten in a more explicit form, namely

$$P_G(t) = \sum_{\ell=1}^{14} M_\ell (1-p)^{m_\ell} p^{5-m_\ell} \delta(t-t_\ell) \quad (24)$$

where the multiplicity factors $\{M_\ell\}$, the exponents $\{m_\ell\}$ and transmissivities $\{t_\ell\}$ are presented in Table I.

As exhibited above, a single scaling transformed the 2 Dirac-delta distribution law of Eq. (21) into the 14 Dirac-delta distribution law of Eq. (24). Under successive scalings, the distribution

law becomes more and more complex, involving a rapidly increasing number of Dirac-delta's. We could in principle follow the evolution, under renormalization, of the distribution law until it attains an invariant form (fixed point). This procedure has in fact been used [35] for random-resistor problems. However an operationally much simpler and numerically excellent procedure can be followed [15] instead, namely to approximate the distribution $P_G(t)$ (Eq. (24)) by a binary one, given by

$$P'(t) = (1 - p')\delta(t - t'_1) + p'\delta(t - t'_2) \quad (25)$$

where p' , t'_1 and t'_2 are completely determined by imposing the preservance of three appropriate momenta. One natural possible choice could be the first three momenta of t (this choice has been tested [15] for the Ising case). Herein we shall adopt instead a more sophisticated choice, namely the first three momenta of $s(t)$ (see definition (19)); this choice has already proved in similar problems [15,22] to be extremely performant from the numerical standpoint.

So, to be precise, we impose

$$\langle s(t) \rangle_{P'} = \langle s(t) \rangle_{P_G} \quad (26.a)$$

$$\langle [s(t)]^2 \rangle_{P'} = \langle [s(t)]^2 \rangle_{P_G} \quad (26.b)$$

$$\langle [s(t)]^3 \rangle_{P'} = \langle [s(t)]^3 \rangle_{P_G} \quad (26.c)$$

hence (by using Eqs. (24) and (25))

$$(1 - p')s_1' + p's_2' = \sum_{\ell=1}^{14} M_{\ell}(1 - p)^{m_{\ell}} p^{5-m_{\ell}} s_{\ell} \equiv F(p, s_1, s_2) \quad (27.a)$$

$$(1 - p')s_1'^2 + p's_2'^2 = \sum_{\ell=1}^{14} M_{\ell}(1 - p)^{m_{\ell}} p^{5-m_{\ell}} s_{\ell}^2 \equiv G(p, s_1, s_2) \quad (27.b)$$

$$(1 - p')s_1'^3 + p's_2'^3 = \sum_{\ell=1}^{14} M_{\ell}(1 - p)^{m_{\ell}} p^{5-m_{\ell}} s_{\ell}^3 \equiv H(p, s_1, s_2) \quad (27.c)$$

where

$$s_k' \equiv s(t_k') \quad (k = 1, 2) \quad (28)$$

and

$$s_{\ell} \equiv s(t_{\ell}) \quad (\ell = 1, 2, \dots, 14) \quad (29)$$

Let us recall (see Table I) that the $\{t_{\ell}\}$ are functions of (t_1, t_2) , and therefore (through definition (19)) functions of $(s_1, s_2) \equiv (s(t_1), s(t_2))$.

The solution of Eqs. (27) is given by

$$p' = \frac{L^2}{1 + L^2} \quad (30.a)$$

$$s_1' = F \pm L\sqrt{K} \quad (30.b)$$

$$s_2' = F \mp \frac{1}{L}\sqrt{K} \quad (30.c)$$

where

$$K \equiv G - F^2 \geq 0 \quad (31)$$

and

$$L \equiv \frac{\sqrt{(H-3FK-F^3)^2 + 4K^3} - (H-3FK-F^3)}{2K^{3/2}} \quad (32)$$

The upper (lower) signs in Eqs. 30.b and 30.c are to be used in the region $s_1 > s_2$ ($s_1 < s_2$) hence $t_1 > t_2$ ($t_1 < t_2$) hence $J_1 > J_2$ ($J_1 < J_2$). Eqs. (30) (together with Eqs. (31) and (32)) are invariant through the $(p, s_1, s_2) \rightleftharpoons (1-p, s_2, s_1)$ transformation and completely determine the RG flow in the $p-s_1-s_2$ space (which determines in turn all the important properties associated with the $p-k_B T/J_2 - \gamma$ space). In particular the calculation of the fixed points and relevant Jacobians

$$J \equiv \begin{pmatrix} \frac{\partial p'}{\partial p} & \frac{\partial p'}{\partial s_1} & \frac{\partial p'}{\partial s_2} \\ \frac{\partial s'_1}{\partial p} & \frac{\partial s'_1}{\partial s_1} & \frac{\partial s'_1}{\partial s_2} \\ \frac{\partial s'_2}{\partial p} & \frac{\partial s'_2}{\partial s_1} & \frac{\partial s'_2}{\partial s_2} \end{pmatrix} \quad (33)$$

is now perfectly feasible.

We have also established, through analytic implementation in computer of the BCM^[21], the full set of equations associated with the $b = 3$ Wheatstone-bridge (Fig. 1(c)); the results are however too lengthy to be quoted here. Let us illustrate this by mentioning that: (i) the analogue of Eq. (22) contains 2^{13} terms (instead of 2^5); (ii) $t_G(r_1, r_2, \dots, r_{13})$ is a rational function whose numerator and denominator respectively contain 765 and 397 different terms (instead of 10 and 5 respectively in Eq. (23)); (iii) the analogue of Eq. (24) contains 2204

terms (instead of 14).

Our main $b = 2$ and $b = 3$ RG results are presented in the next Section.

IV- RESULTS

Both $b = 2$ and $b = 3$ present RG's provide the following results (see Figs. 2 and 3) which are in fact expected to be common to all values of b :

- i) the points $(p, s_1, s_2) = (0, 0, 0)$ and $(1, 1, 1)$ are fully stable fixed ones, respectively corresponding to the $T \rightarrow \infty$ (paramagnetic phase) and $T \rightarrow 0$ (ferromagnetic phase) limits;
- ii) the points $(0, 0, 1)$, $(1, 0, 0)$, $(1, 1, 0)$, $(0, 1, 0)$, $(1, 0, 1)$ and $(0, 1, 1)$ are semistable fixed ones (the first three belong to the paramagnetic region; the second three to the ferromagnetic one);
- iii) in the critical surface (the hexagon-like one in the interior of the unit cube in Fig. 2.(a)) the points $(1/2, 0, 1)$ and $(1/2, 1, 0)$ are fully unstable fixed ones, corresponding to the bond percolation limit, and located at the exact position $p_c = 1/2$ (see Eq. (4));
- iv) in the critical surface, the twisted H-like region determined by $(s_1 = s_2 = 1/2, \forall p)$, $(s_1 = 1/2, p = 0, \forall s_2)$ and $(s_2 = 1/2, p = 1, \forall s_1)$ corresponds to the pure Potts model, and its location is the exact one (see Eq. (3)); three fixed points (namely $(p, s_1, s_2) = (1/2, 1/2, 1/2)$, $(0, 1/2, 1/2)$ and $(1, 1/2, 1/2)$) are found which belong to this region. If we restrict our-

selves to the analysis of the RG flow in the critical surface, the fixed points $(p, s_1, s_2) = (0, 1/2, 1/2)$ and $(1, 1/2, 1/2)$ are semistable whereas the central one $(p = s_1 = s_2 = 1/2)$ is fully stable for $q \leq q^*(b)$ ($q^*(2) \simeq 5.3$ and $q^*(3) \simeq 4.9$) but becomes semistable for $q > q^*(b)$ (see point (v) below and Figs. 1(b)-(e)).

v) in the critical surface, the straight line $s_1 + s_2 = 1$ at $p = 1/2$ flows within itself, corresponds to the equal concentration model and recovers the exact result (see Eq. (5)); this line contains the central point $p = s_1 = s_2 = 1/2$ which, as said in point (iv), attracts, for $q \leq q^*(b)$, every one of its points, (it attracts in fact all the points of the critical surface, excepting the bond percolation points and the pure Potts $(p, s_1, s_2) = (0, 1/2, 1/2)$ and $(1, 1/2, 1/2)$ ones); this central point becomes unstable at $q = q^*(b)$ and bifurcates (in pitchfork manner; see Fig. 4) into two new fixed points (which, for $q > q^*(b)$, play the attracting role within the critical surface) located at $(p, s_1, s_2) = (1/2, s_r, 1 - s_r)$ and $(1/2, 1 - s_r, s_r)$ (r stands for random; see Figs. 2(d), 2(e) and (4); the $q \rightarrow q^*(b)$ limit presents an interesting behavior, namely that $s_r(q) - 1/2 \sim A [q/q^*(b) - 1]^{1/2}$ where $A \simeq 0.29$ for both $b = 2$ and $b = 3$, thus suggesting a quasi-universal (independent from b) curve, which in the $b \rightarrow \infty$ limit could be $s_r(q) - 1/2 \sim A(q/2 - 1)^{1/2}$.

vi) the $q = 1$ critical surface is given by

$$(1 - p)s_1 + ps_2 = 1/2 \quad (34)$$

which coincides with both the $q \rightarrow 1$ case of Eq. (9), and the exact result (see Eq. (6)).

We shall now focus the Jacobians (see Eq. (53)) associated with the fixed points we have mentioned.

- i) At the $(0,0,0)$ and $(1,1,1)$ fixed points the respective Jacobians identically vanish for all values of q , thus indicating that their stability is due to higher order terms.
- ii) At the semi-stable fixed points $(1,0,1)$, $(1,1,0)$ and $(1,0,0)$ the Jacobians are given respectively by

$$\begin{pmatrix} 0 & 0 & 0 \\ 0 & 2 & 0 \\ 0 & 0 & 0 \end{pmatrix}$$

$$\begin{pmatrix} 0 & 0 & 0 \\ 0 & 0 & 0 \\ 0 & 2 & 0 \end{pmatrix}$$

and

$$\begin{pmatrix} g & 0 & 0 \\ 0 & 0 & 0 \\ 0 & 0 & 0 \end{pmatrix}$$

where $g \simeq 4$ for all values of q (the Jacobians corresponding to the $(0,1,0)$, $(0,0,1)$ and $(0,1,1)$ fixed points are analogous). As above we verify that the stability is related to higher order terms.

- iii) The Jacobian at the percolation fixed points independes from q , and is proportional to unity (therefore the crossover exponent ϕ_p equals 1, thus recovering the exact result expressed in Eq. (14)); the three times degenerate eigenvalue λ_p equals 1.62500, 2.21729, 2.76579 and 3.27894 for $b = 2, 3, 4$ and 5 respectively (the values associated with $b = 4, 5$ have been calculated as well; see also Ref. [21]). Through the RG expression $\nu_p(b) = \ln b / \ln \lambda_p(b)$ we obtain the results indicated in Table II ($q=1$ column)
- iv) The Jacobian associated with the pure Potts central fixed point ($p=s_1=s_2=1/2$) presents the following simple structure:

$$\begin{pmatrix} a(q) & 0 & 0 \\ 0 & b(q) & c(q) \\ 0 & c(q) & b(q) \end{pmatrix} \quad (35)$$

where $a(q) \simeq 0.5$ for all values of q in the range $[1, 10]$. The other two eigenvalues (respectively associated with the eigenvectors $(0, 1, -1)$ and $(0, 1, 1)$) are $\lambda'(q) \equiv b(q) - c(q)$ and $\lambda_t(q) \equiv b(q) + c(q)$; $\lambda'(q)$ depends slowly on q , it is smaller (higher) than unity for $q < q^*(b)$ ($q > q^*(b)$) and, at the bifurcation point, it satisfies $\lambda'(q^*(b)) = 1$. $\lambda_t(q)$ is always higher than unity, and is given by

$$\lambda_t(q) = \frac{8 + 13q^{1/2} + 5q}{8 + 7q^{1/2} + q} \quad (b=2) \quad (36.a)$$

$$\lambda_t(q) = \frac{576 + 2092q^{1/2} + 3051q + 2272q^{3/2} + 901q^2 + 177q^{5/2} + 13q^3}{576 + 1388q^{1/2} + 1323q + 632q^{3/2} + 157q^2 + 19q^{5/2} + q^3} \quad (b = 3) \quad (36.b)$$

$$\begin{aligned} \lambda_t(q) = & \frac{161128382464 + 1697859502080q^{1/2} + 8483753136128q + 26753044992000q^{3/2}}{161128382464 + 1447535050752q^{1/2} + 6179539095552q + 16682662418944q^{3/2}} \\ & + \frac{59776725996784q^2 + 100721482408584q^{5/2} + 132981697848499q^3}{31974143639184q^2 + 46299588621448q^{5/2} + 52626772572121q^3} \\ & + \frac{141113527133368q^{7/2} + 122475851169593q^4 + 88012263034920q^{9/2}}{48157988221974q^{7/2} + 36100260892173q^4 + 22438276696524q^{9/2}} \\ & + \frac{52807853404826q^5 + 26600381596312q^{11/2} + 11282937714602q^6}{11660435998306q^5 + 5093660852058q^{11/2} + 1876055420530q^6} \\ & + \frac{4033410386968q^{13/2} + 1213716439993q^7 + 306427439732q^{15/2} + 64547996440q^8}{583142336798q^{13/2} + 152826115979q^7 + 33671740016q^{15/2} + 6206221404q^8} \\ & + \frac{11251035116q^{17/2} + 1603874125q^9 + 183922732q^{19/2} + 16564782q^{10} + 1129660q^{21/2}}{949837808q^{17/2} + 119415951q^9 + 12142442q^{19/2} + 975746q^{10} + 59778q^{21/2}} \\ & + \frac{54907q^{11} + 1696q^{23/2} + 25q^{12}}{2629q^{11} + 74q^{23/2} + q^{12}} \quad (b = 4) \quad (36.c) \end{aligned}$$

By using Eqs. (36) we have obtained the results for ν_t indicated in Table II (the $b = 5$ case has been treated numerically). Furthermore the crossover exponent $\phi \equiv \ln \lambda' / \ln \lambda_t$ (associated with the appearance of a new universality class due to bond randomness) has also been calculated: the results are presented in Fig. 5.

We recall that with the pure Potts model two other fixed points (namely $(p, s_1, s_2) = (0, 1/2, 1/2)$ and $(1, 1/2, 1/2)$) are associated. The corresponding Jacobians are respectively

$$\begin{pmatrix} d(q) & 0 & 0 \\ 0 & \lambda_t(q) & 0 \\ 0 & \lambda_t(q) - e(q) & e(q) \end{pmatrix} \quad (37.a)$$

and

$$\begin{pmatrix} d(q) & 0 & 0 \\ 0 & e(q) & \lambda_t(q) - e(q) \\ 0 & 0 & \lambda_t(q) \end{pmatrix} \quad (37.b)$$

where the eigenvalue $d(q) > 1$, $\forall q$ (its eigenvector is $(1, 0, 0)$), the eigenvalue $e(q)$ satisfies $0 < e(q) < 1$, $\forall q$ (its eigenvector is $(0, 0, 1)$ for the $p = 0$ fixed point and $(0, 1, 0)$ for the $p = 1$ one), and the eigenvalue $\lambda_t(q)$ is given by Eqs. (36) (its eigenvector is $(0, 1, 1)$).

- v) The Jacobian associated with the random fixed points (namely $(p, s_1, s_2) = (1/2, s_r, 1 - s_r)$ and $(1/2, 1 - s_r, s_r)$) presents no symmetry at all, its 9 elements are non vanishing and different among them, the eigenvectors constitute a fully non orthogonal basis, and its eigenvalues are $\lambda_1(q)$ (it smoothly decreases from about 0.5 to about 0.3 when q increases from $q^*(b)$ to 10; its associated eigenvector is roughly along the $(1, 0, 0)$ direction), $\lambda_2(q)$ (it smoothly de-

creases from 1 to about 0.8 when q increases from $q^*(b)$ to 10), and $\lambda_3(q) \equiv \lambda_r(q)$ (it smoothly decreases from about 2.2 to about 2 when q increases from $q^*(b)$ to 10; its associated eigenvector is roughly along the (0,1,1) direction). From $\lambda_r(q)$ we can calculate the correlation length critical exponent $\nu_r = \ell n b / \ell n \lambda_r$ corresponding to the new universality class (see Fig. 6). By using the scaling relation $2 - \alpha(q) = d \nu(q)$ ($d = 2$) we can calculate the discrepancy $\alpha_t - \alpha_r$ for $q > q^*$ (as long as we do not attain the first order transition regime); see Fig. 7. Our results are sensibly different from those obtained by Kinzel and Domany^[10]. While our difference $\alpha_t - \alpha_r$ monotonously increases with α_t , theirs presents a maximum; furthermore the scales are quite different, as our results suggest that $\alpha_t(\text{exact}) - \alpha_r(\text{exact})$ is (for $q > 2$ and second order transitions) roughly proportional to $\alpha_t(\text{exact})$ with a proportionality coefficient close to unity, while they obtain differences about 10 times smaller. Our suggestion ($\alpha_t - \alpha_r \simeq \alpha_t$) implies $\alpha_r \simeq 0$ for $2 \leq q \leq 4$, which is perfectly consistent with both Monte Carlo^[12] and experimental^[36] data^[13,14].

In Fig. 8 we present, as functions of size b , the values we obtain for $q^*(b)$ (where the bifurcation appears) and for $q_c(b)$ (where $\alpha_t(b)$ vanishes or equivalently $\nu_t(b) = 1$). We verify that Harris criterion^[11] ($q^*(b) = q_c(b)$ in the present language) is not satisfied for finite size clusters. As this criterion refers to macroscopic systems, one can speculate that $\lim_{b \rightarrow \infty} q^*(b) = \lim_{b \rightarrow \infty} q_c(b) (= 2, \text{ in the present case})$.

With respect to the derivatives associated with the diluted case ($J_1=0$, i.e. $s_1=0$) we obtain (for all b in fact) $(ds_2/dp)_{p=1/2} = -2$, $\forall q$, which recovers the exact result expressed in Eq. (8). The derivatives obtained in the $p \rightarrow 1$ limit are indicated in Table III: small errors are unfortunately present for $q \neq 1$.

Typical numerical results obtained through the $b=2$ RG are presented in Tables IV and V. The $q=2$ case recovers the results obtained through the s -RG of Ref. [15]. Note in Table IV that the critical surface in the p - s_1 - s_2 space is almost independent from q , and very close to that determined by Eq. (9) (i.e. $(1-p)s_1 + ps_2 = 1/2$). The great quantity of exact results (in fact, among those presently known for the critical surface, all but one derivative analysed in Table III) that are recovered by the present RG tends to support the numerical results as being high precision ones. We estimate (see also Ref. [15]) that the results presented in Table IV (and consistently in Table V) are exact everywhere within an error in s_2 less than 10^{-3} (error which is attained only in the worse region, most probably the neighborhood of $(p, s_1) \simeq (0.8, 0.25)$).

V - CONCLUSION

We have discussed several aspects of the criticality of the quenched bond-mixed q -state Potts ferromagnet in square lattice. The analysis has been done within a real space re-

normalization group (RG) framework by using two-terminal self-dual clusters which have already proved to be extremely performant for the square lattice, although rigorously speaking they are to be related to a (self-dual) hierarchical lattice. Through the renormalization operations the coupling constant distribution law (originally binary) quickly evolves into a multi-delta distribution. Rather than following this distribution until arrival into a fixed form, we have re-established the binary form by imposing the preservall of the first three momenta (we recall that our model has three free parameters) of a quite convenient variable (the s -variable).

The present RG recovers several exact results already available in the literature, such as the critical points corresponding to bond percolation, pure Potts and equal concentration models, as well as the $T \rightarrow 0$ limit asymptotic behavior of the critical line associated with the bond-dilute case, the percolation crossover critical exponent ϕ_p and the $q \rightarrow 1$ limit critical point (e.i. it satisfies the Kasteleyn and Fortuin theorem).

The present treatment introduces a small error (which, for cluster size $b = 2$, grows from 0% to 1.5% while q increases from 1 to 4) in the $p \rightarrow 1$ limit derivative of the critical line associated with the bond-dilute particular case, as well as in the correlation length critical exponent ν_t (which, for cluster size $b = 5$, grows from 1.6% to 34.5% while q increases from 1 to 4). The growing of the errors when we approach $q = 4$ comes from the fact that the present RG does not reproduce the appearance of the first-order transition regime (expected at least

for the pure case); to overcome this difficulty larger parameter space would have to be considered.

Let us finally summarize the main aspects that have received some improvement within our discussion:

- (i) the critical temperatures associated with arbitrary values of concentration p and ratio J_1/J_2 have been numerically established with high precision (the error in the s -variable being less than 10^{-3} in the worse region); the results are, for $1 \leq q \leq 4$, consistently recovered by the simple analytic approximation expressed in Eq. (9) ^[5];
- (ii) when q increases above a critical value q^* (expected to be $q^* = 2$ for macroscopic systems), a new type of fixed point (namely the random fixed point) appears through a pitchfork bifurcation, and consequently the random model enters into a new universality class (as long as the first-order transition regime is not attained); the bifurcation does not occur simultaneously with the vanishing of the specific heat critical exponent α_t of the pure model, and therefore the Harris criterion appears to be intimately related to the thermodynamic limit, as only in the $b \rightarrow \infty$ limit it could possibly be recovered;
- (iii) the random specific heat critical exponent α_r is close to zero for all values above q^* , which is consistent with available Monte Carlo ^[12] and experimental ^[36] data for the $q = 4$ case;
- (iv) the q -dependence (above q^*) of the pure to random crossover critical exponent ϕ_t is approximately established.

Treatments of the random Potts ferromagnet simultaneous ly incorporating both pure-random crossover and second-first order regime change ment would be very welcome.

We acknowledge useful discussions with E.F. Sarmiento, E. M.F. Curado, G. Schwachheim and M. Schick; one of us (C.T.) also acknowledges interesting remarks from R.B. Stinchcombe and P. Beale. U.M.S.C. has benefitted from a CAPES Fellowship (Brazilian Agency); C.T. benefitted from partial support through a Guggenheim Fellowship tenure.

REFERENCES

- [1] F.Y.Wu, Rev. Mod. Phys. 54, 235 (1982)
- [2] B.W.Southern and M.F.Thorpe, J. Phys. C 12, 5351 (1979)
- [3] L.Turban, J. Phys. C 13, L13 (1980)
- [4] C.Tsallis and A.C.N. de Magalhães, J. Physique 42, L227 (1981)
- [5] C.Tsallis, J. Phys. C 14, L85 (1981)
- [6] A.C.N. de Magalhães and C.Tsallis, J. Phys. 42, 1515 (1981)
- [7] S.Sarbach and F.Y.Wu, Z. Phys. B 44, 309 (1981)
- [8] R.J.V. dos Santos and C.Tsallis, J. Phys. A 16 (1983, under press)
- [9] J.M.Yeomans and R.B. Stinchcombe, J. Phys. C 13, L239 (1979)
- [10] W.Kinzel and E. Domany, Phys. Rev. B 23, 3421 (1981)
- [11] A.B.Harris, J. Phys. C 7, 1671 (1974)
- [12] M.A.Novotny and D.P.Landau, Phys. Rev. B 24, 1468 (1981)
- [13] L.D.Roelofs, N.C.Bartelt and T.L.Einstein, Phys. Rev. Lett. 47, 1348 (1981)
- [14] F.Family, Phys. Rev. Lett. 48, 367 (1982)
- [15] S.V.F.Levy, C.Tsallis and E.M.F.Curado, Phys. Rev. B 21, 2991 (1980)
- [16] P.W.Kasteleyn and C.M.Fortuin, J. Phys. Soc. Japan (Suppl.) 26, 11 (1969)
- [17] R.J.Baxter, J. Phys. C 6, L445 (1973); B.Nienhuis, A.N. Berker, E.K.Riedel and M.Schick, Phys. Rev. Lett. 43, 737 (1979)
- [18] M.P.M. den Nijs, J. Phys. A 12, 1857 (1979); J.Black and V.J.Emery, Phys. Rev. B 23, 429 (1981); J.L.Cardy, M. Nauenberg and D.J.Scalapino, Phys. Rev. B 22, 2560 (1980)
- [19] D.J.Wallace and A.P.Young, Phys. Rev. B 17, 2384 (1977); A.Coniglio, Phys. Rev. Lett. 46, 250 (1981)

- [20] C.Domb, J. Phys. A 7, 1335 (1974)
- [21] C.Tsallis and S.V.F.Levy, Phys. Rev. Lett. 47, 950 (1981)
- [22] A.C.N. de Magalhães, G.Schwachheim and C.Tsallis, J. Phys. C 15, 6791 (1982)
- [23] J.Bernasconi, Phys. Rev. B 18, 2185 (1978)
- [24] C.J.Lobb, D.J.Frank and M.Tinkham, Phys. Rev. B 23, 2262 (1981)
- [25] S.W.Kenkel and J.P.Straley, Phys. Rev. Lett. 49, 767 (1982)
- [26] C.Tsallis, A.Coniglio and S.Redner, J. Phys. C 16, 4339 (1983)
- [27] P.J.Reynolds, W.Klein and H.E.Stanley, J. Phys. C 10, L167 (1977)
- [28] A.C.N. de Magalhães, C.Tsallis and G.Schwachheim, J. Phys. C 13, 321 (1980)
- [29] J.M.Yeomans and R.B.Stinchcombe, J. Phys. C 12, L169 and 347 (1979)
- [30] E.M.F.Curado, C.Tsallis, S.V.F.Levy and M.J. de Oliveira, Phys. Rev. B 23, 1419 (1981)
- [31] H.O.Mártin and C.Tsallis, J. Phys. C. 14, 5645 (1981)
- [32] A.O.Caride, C.Tsallis and S.I.Zanette, Phys. Rev. Lett. 51, 145 (1983)
- [33] H.O.Mártin and C.Tsallis, J.Phys. C 16, 2787 (1983)
- [34] J.W.Essam, preprint (1982)
- [35] A.P.Young and R.B.Stinchcombe, J. Phys. C 9, 4419 (1976)
- [36] L.D.Roelofs, A.R.Kortan, T.L.Einstein and R.L.Park, Phys. Rev. Lett. 46, 1465 (1961)

CAPTION FOR FIGURES AND TABLES

- Fig. 1 - Self-dual two-rooted graphs: \bullet (o) denotes internal (terminal) node.
- Fig. 2 - RG flow in the (p, s_1, s_2) space (the arrows indicate the sense of flow). (a) critical surface (heavy lines) separating the para (P) and ferro (F) magnetic phases; it is invariant under the $(p, s_1, s_2) \rightarrow (1-p, s_2, s_1) \rightarrow (p, 1-s_1, 1-s_2)$ transformations, and depends very slightly on q (let us say for $q \geq 1$) and on the RG linear scaling factor b ; the twisted H-like region corresponds to the pure ferromagnet; the $p = 1/2$ line constitutes an invariant subspace corresponding to the equal concentration model; \circ , \bullet and \blacksquare respectively denote fully stable, fully unstable and semi-stable fixed points; the central fixed point $(1/2, 1/2, 1/2)$ bifurcates along the $p = 1/2$ critical line for $q \geq q^*$. (b) and (d) ((c) and (e)) are projections on the (p, s_2) ((p, s_1)) subspace of the critical surface RG flow; (b) and (c) ((d) and (e)) correspond to $q < q^*$ ($q > q^*$); \square denotes the new semi-stable fixed point generated through the bifurcation; the dashed lines correspond to the bond-dilute model.
- Fig. 3 - RG ($b=2$) critical temperature as a function of J_2 -concentration p for typical values of q and J_1/J_2 (numbers parametrizing the curves).
- Fig. 4 - Position of the fixed points which attract almost every point of the critical surface (b denotes the RG linear scaling factor).

- Fig. 5 - q -dependence of the pure to random crossover critical exponent ϕ ; b denotes the RG linear scaling factor; q^* denotes the bifurcation value of q (see Fig. 4).
- Fig. 6 - q -dependence of the RG ($b = 2$) pure (—) and random (—·—·) critical exponents ν_t and ν_r compared to the exact pure (-----) value [18]. For $b = 2$ $q^* \simeq 5.3$; for the exact case we have assumed $q^* = 2$ (we recall that for $q > 4$ the phase transition corresponding to the pure model is a first order one).
- Fig. 7 - Discrepancy between pure and random critical exponents α_t and α_r as a function of the discrepancy $\alpha_t(q) - \alpha_t(q^*)$: our RG ($b = 2$) result (—) compared to that (-----) obtained from Ref. [10] (the exact $\alpha_r(q)$ is still unknown).
- Fig. 8 - Variations of the bifurcation value q^* and the $\alpha = 0$ value q_c as functions of the RG linear scaling factor b . The dashed lines are speculative ones assuming the Harris criterion to be recovered (i.e. $q^* = q_c = 2$) in the $b \rightarrow \infty$ limit.
- Table I - Elements of the distribution $P_G(t)$ (Eq. (24)) associated with the graph of Fig. 1(b) ($q = 2$ recovers Eq. (4) of Ref. [15]).
- Table II - RG and exact [18] critical exponent ν for the pure q -state Potts model (b denotes the linear scaling factor). This Table is consistent (through $2 - \alpha = 2\nu$) with Table 1 of Ref. [33]
- Table III - RG ($b = 2$) results associated with the dilute model (both percolation and pure model critical points as

well as the asymptotic behavior at $T \rightarrow 0$ are ex-
actly recovered for all q)

Table IV - Value for s_2 on the RG ($b = 2$) critical surface, for typical values of (p, s_1) . Note the quasi-independence with respect to q .

Table V - Values of p on the same critical surface appearing in Table IV, for typical values of J_1/J_2 and $k_B T/qJ_2$.

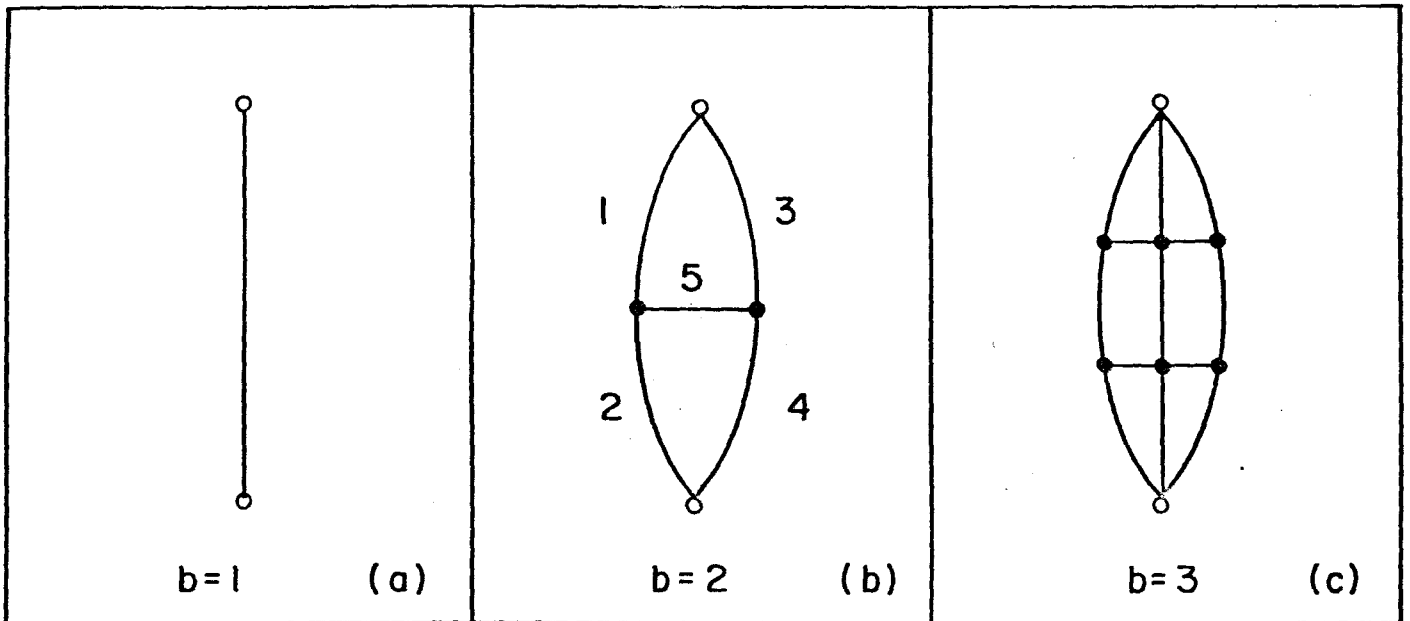


FIG. 1

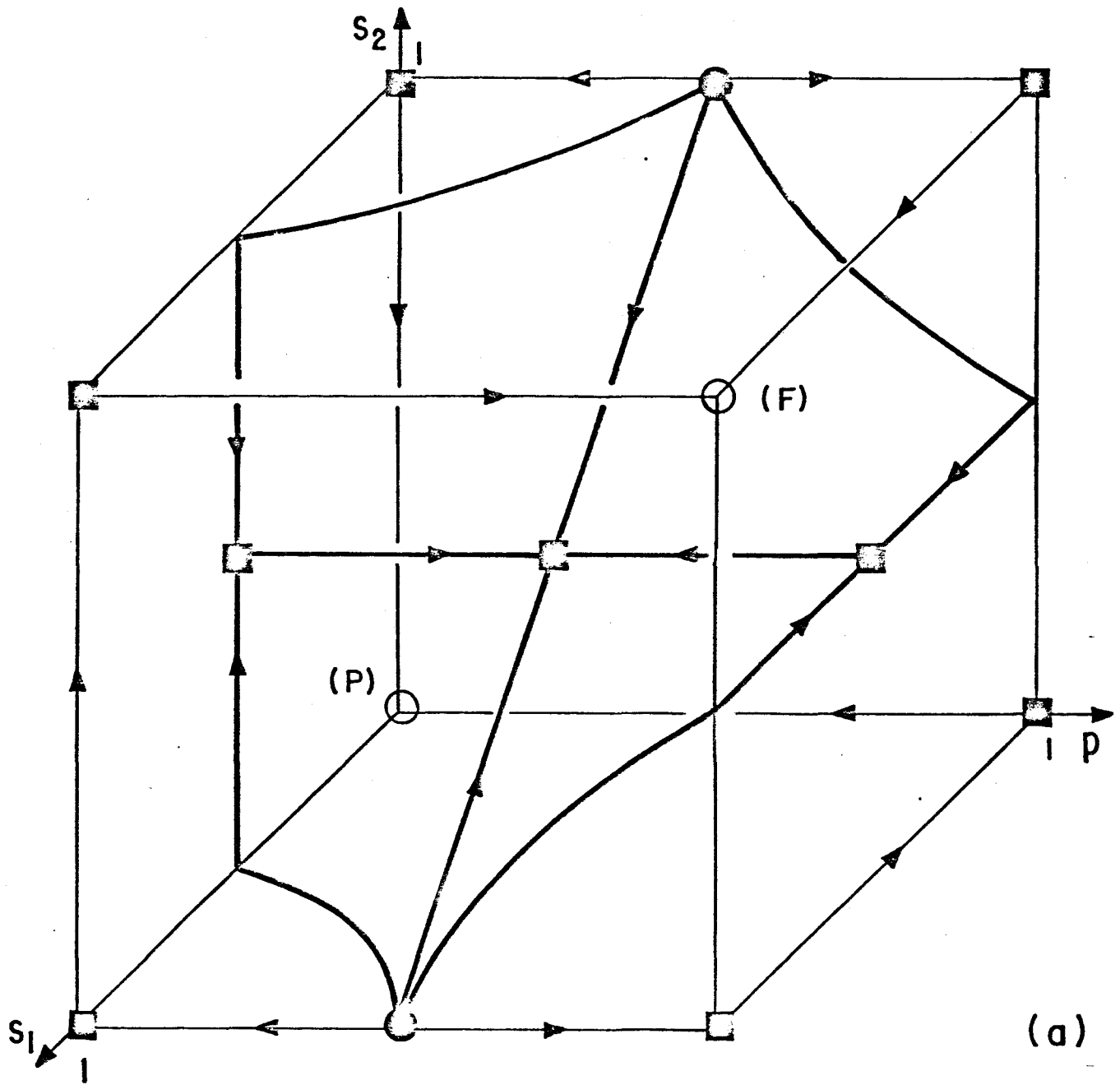
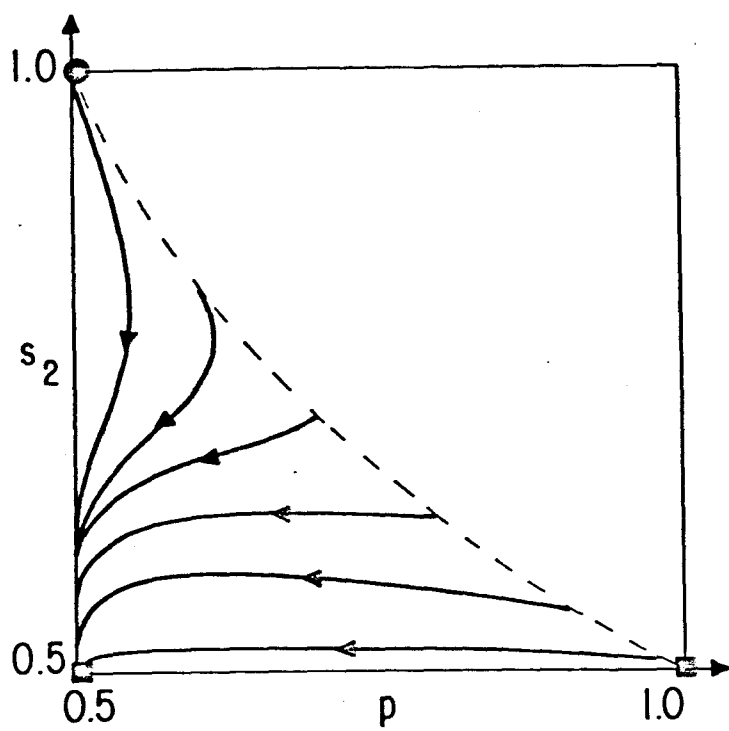
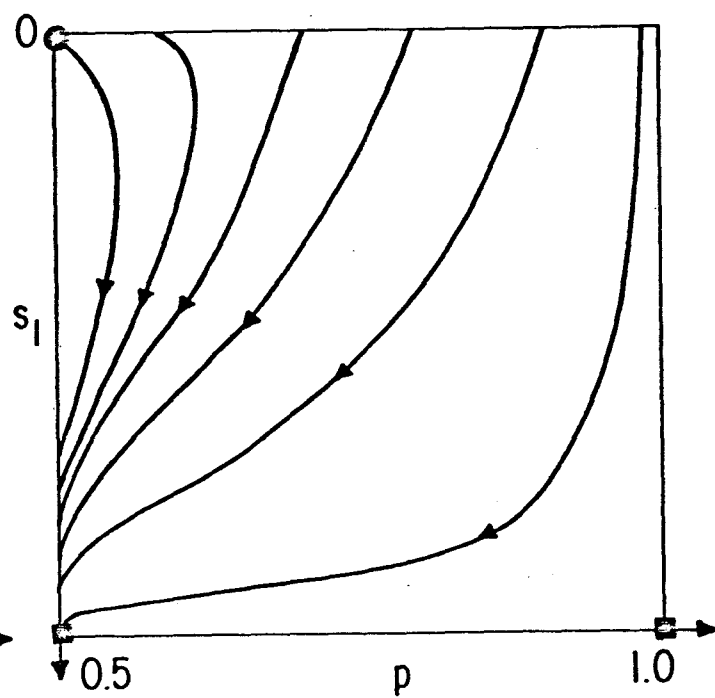


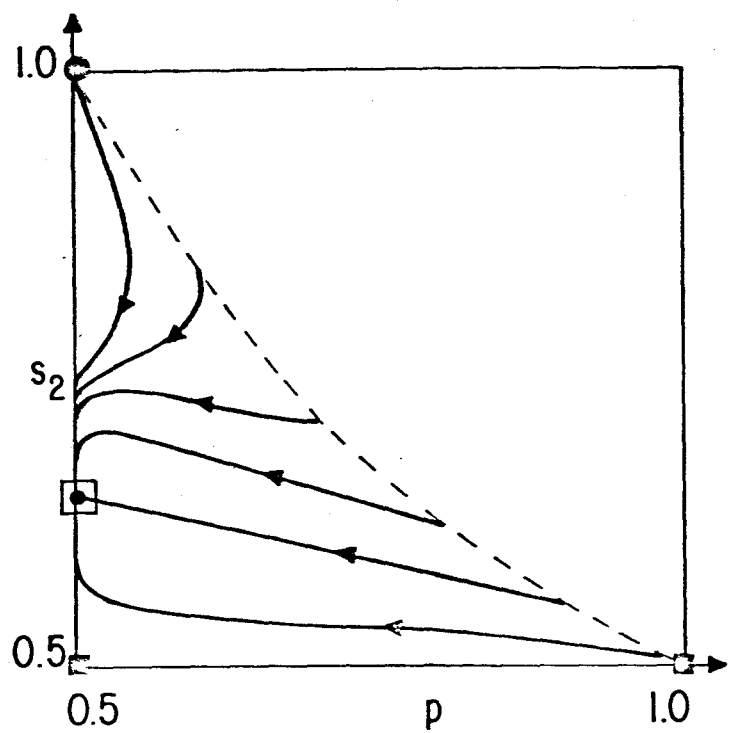
FIG. 2



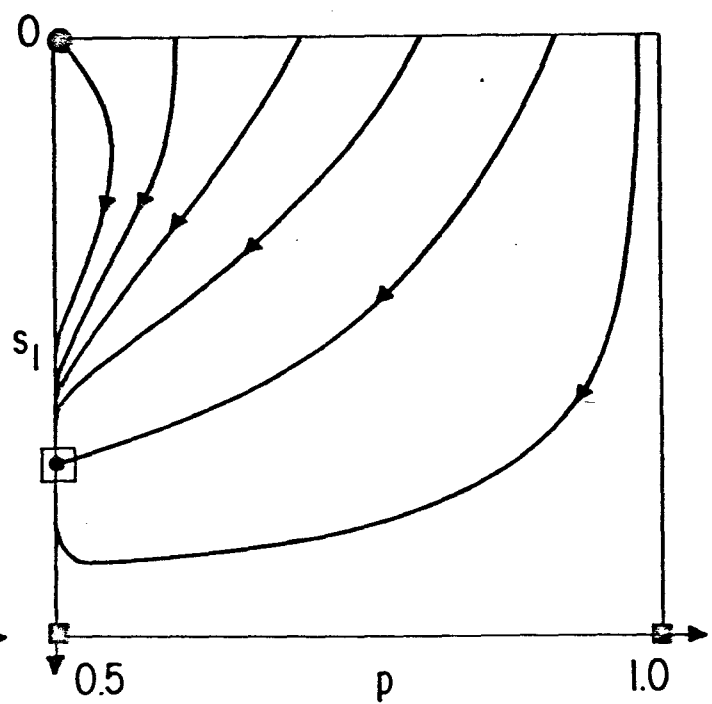
(b)



(c)



(d)



(e)

FIG. 2

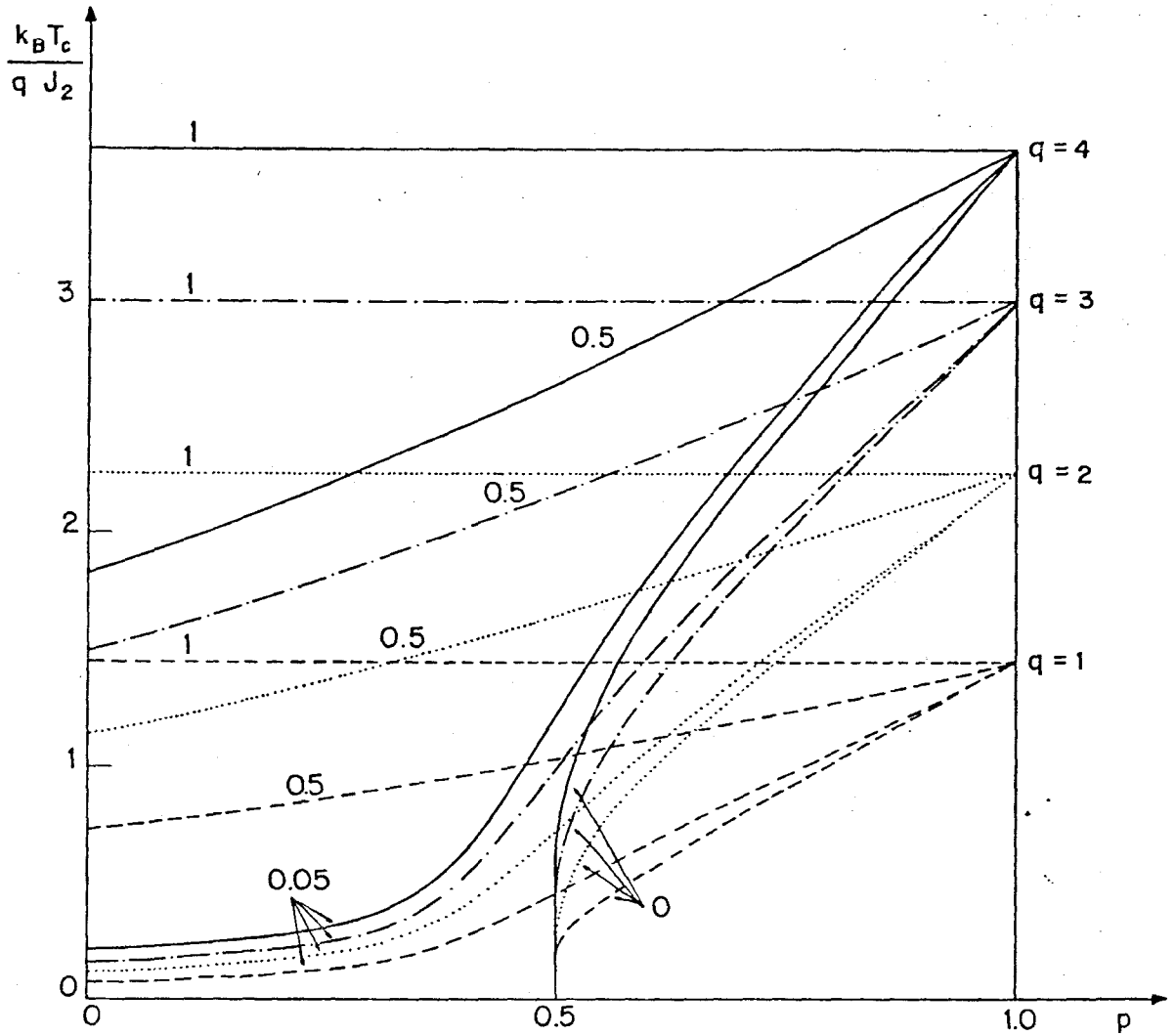


FIG. 3

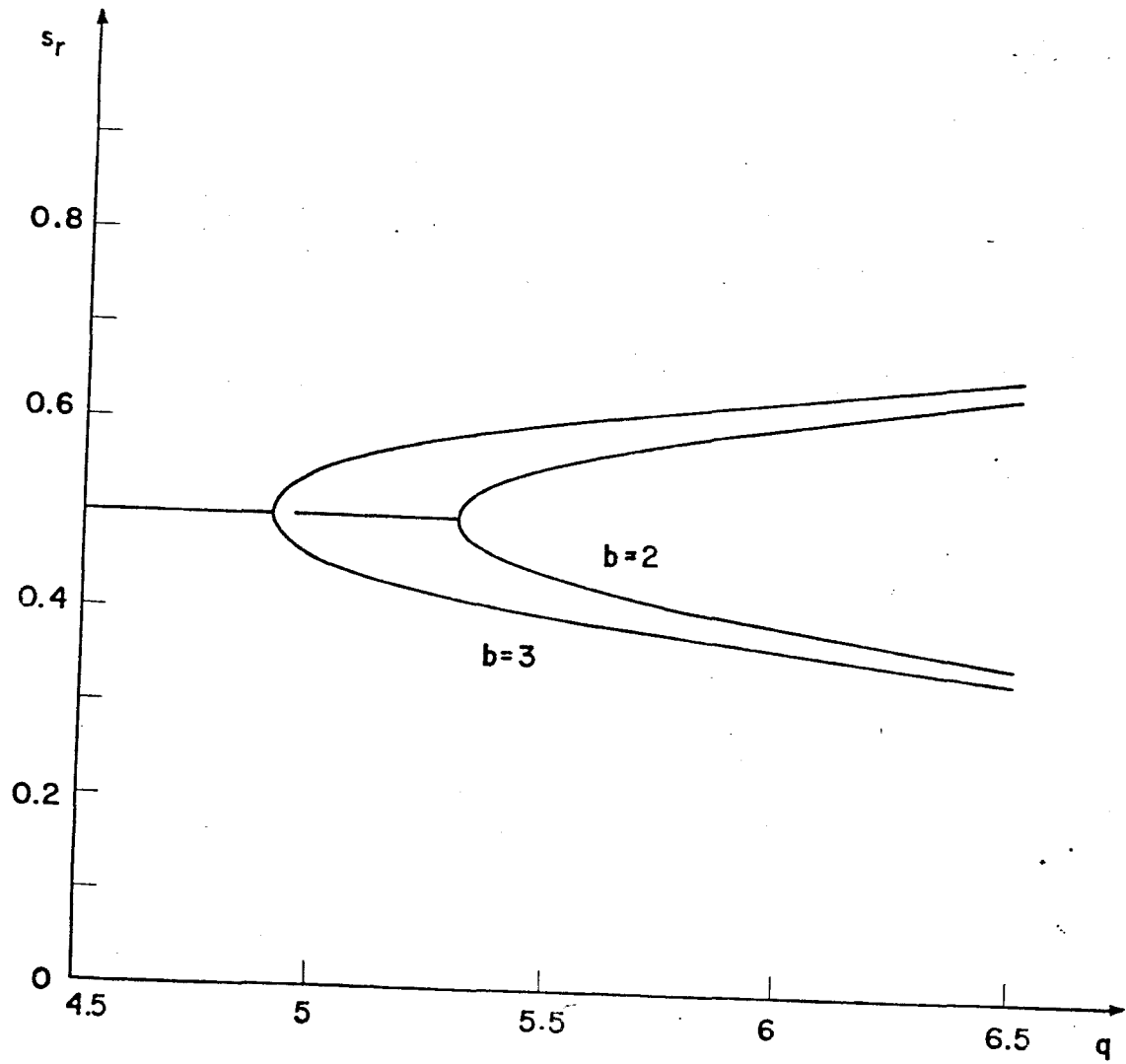


FIG. 4

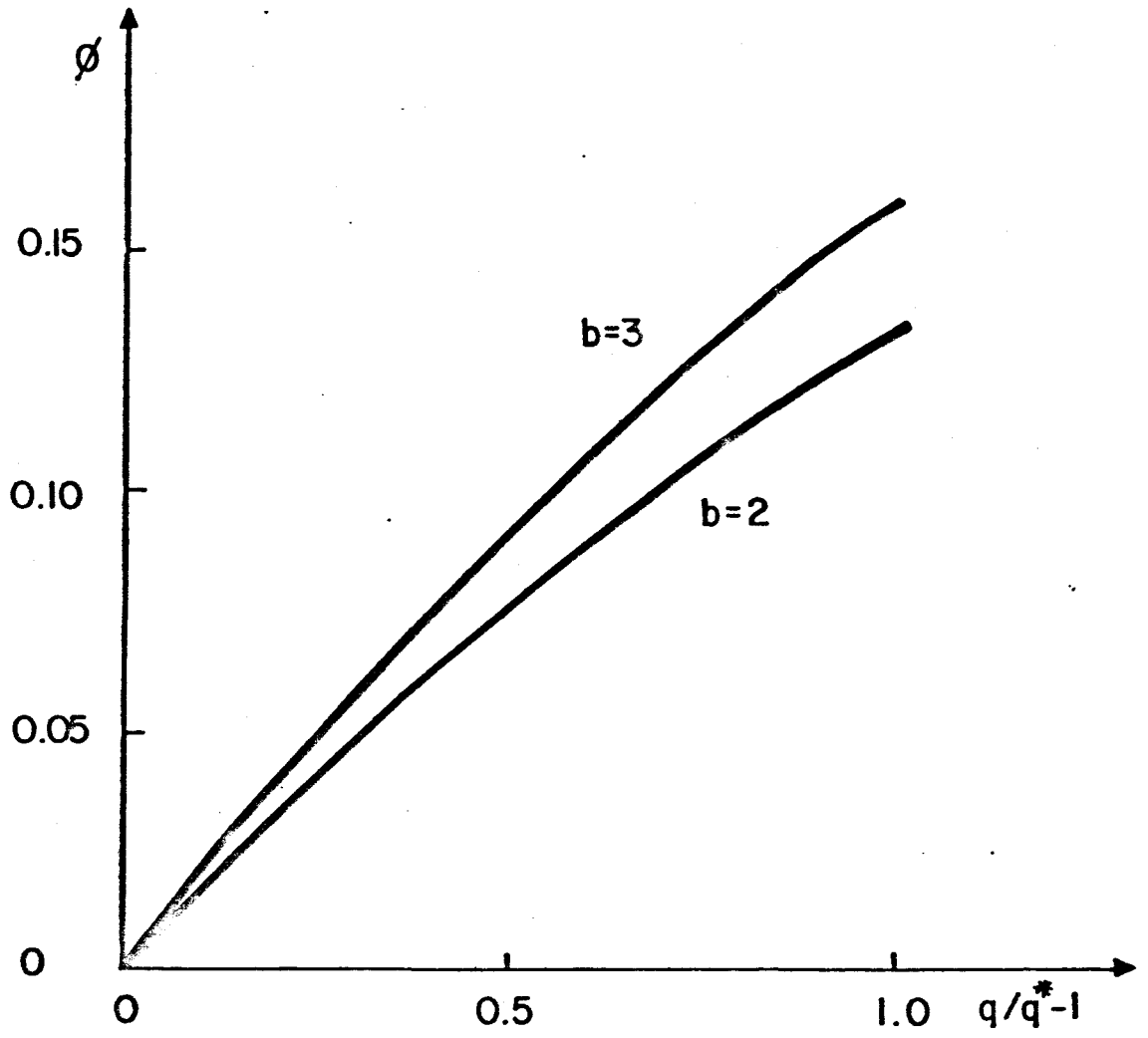


FIG. 5

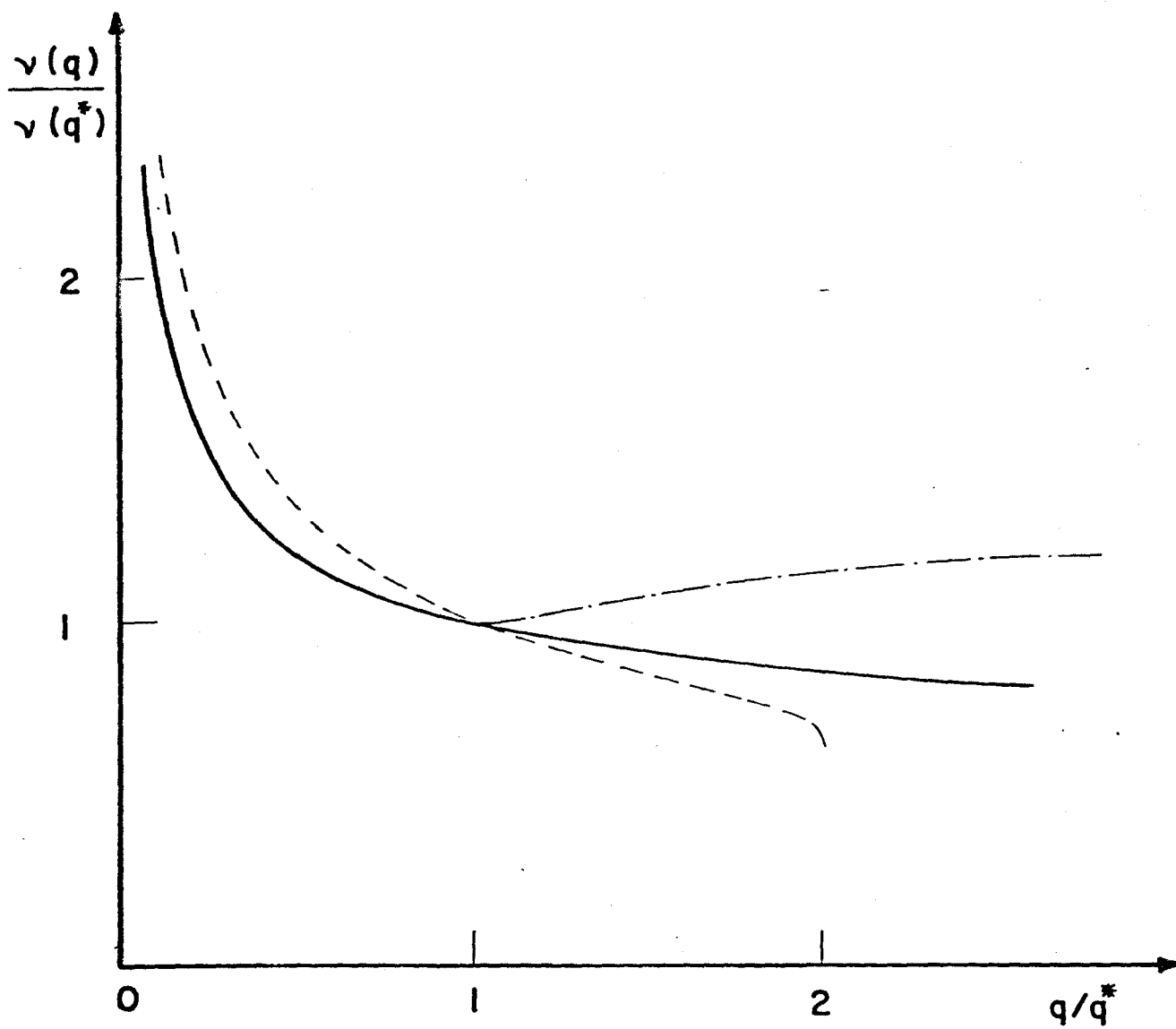


FIG.6

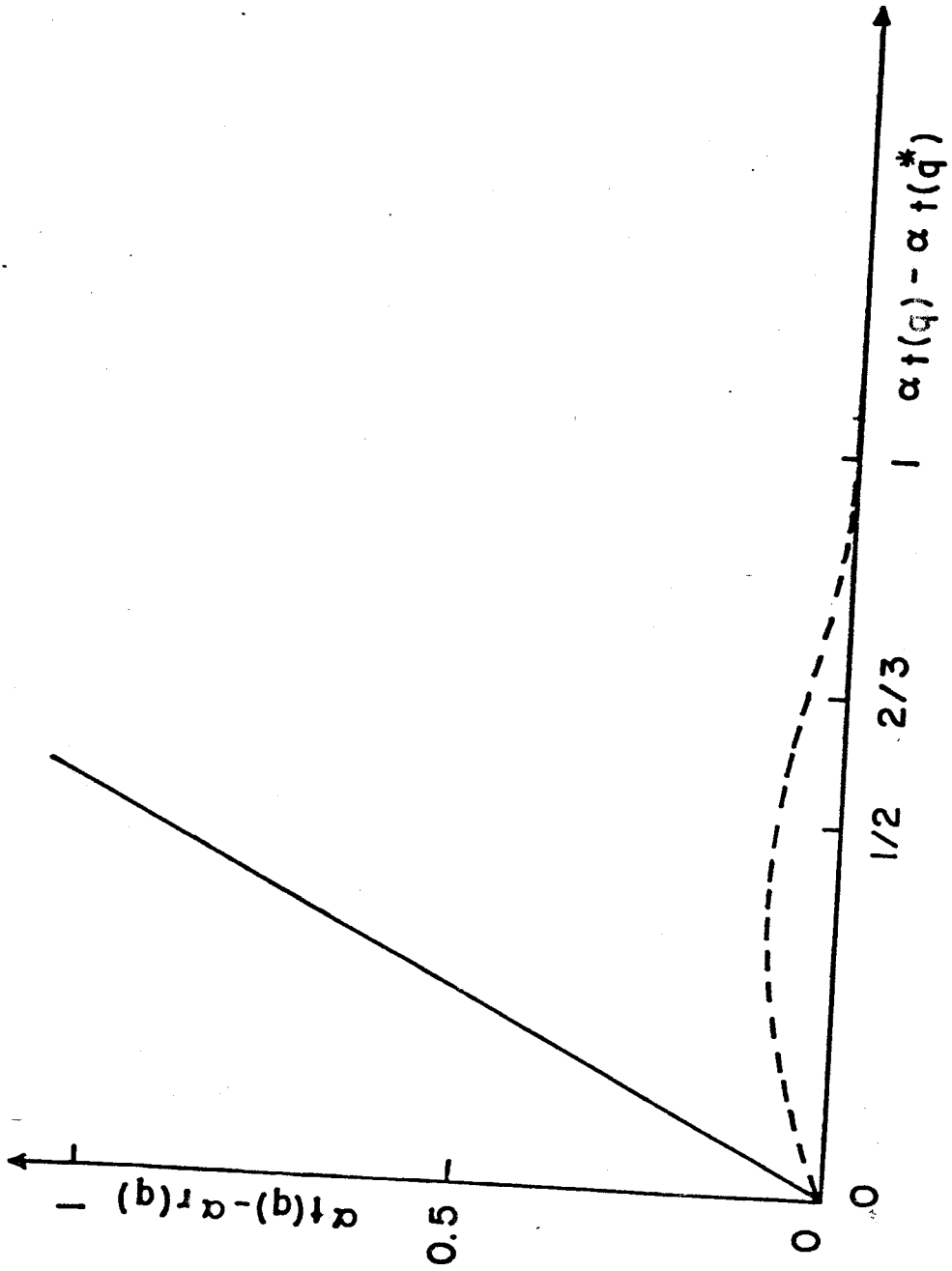


FIG. 7

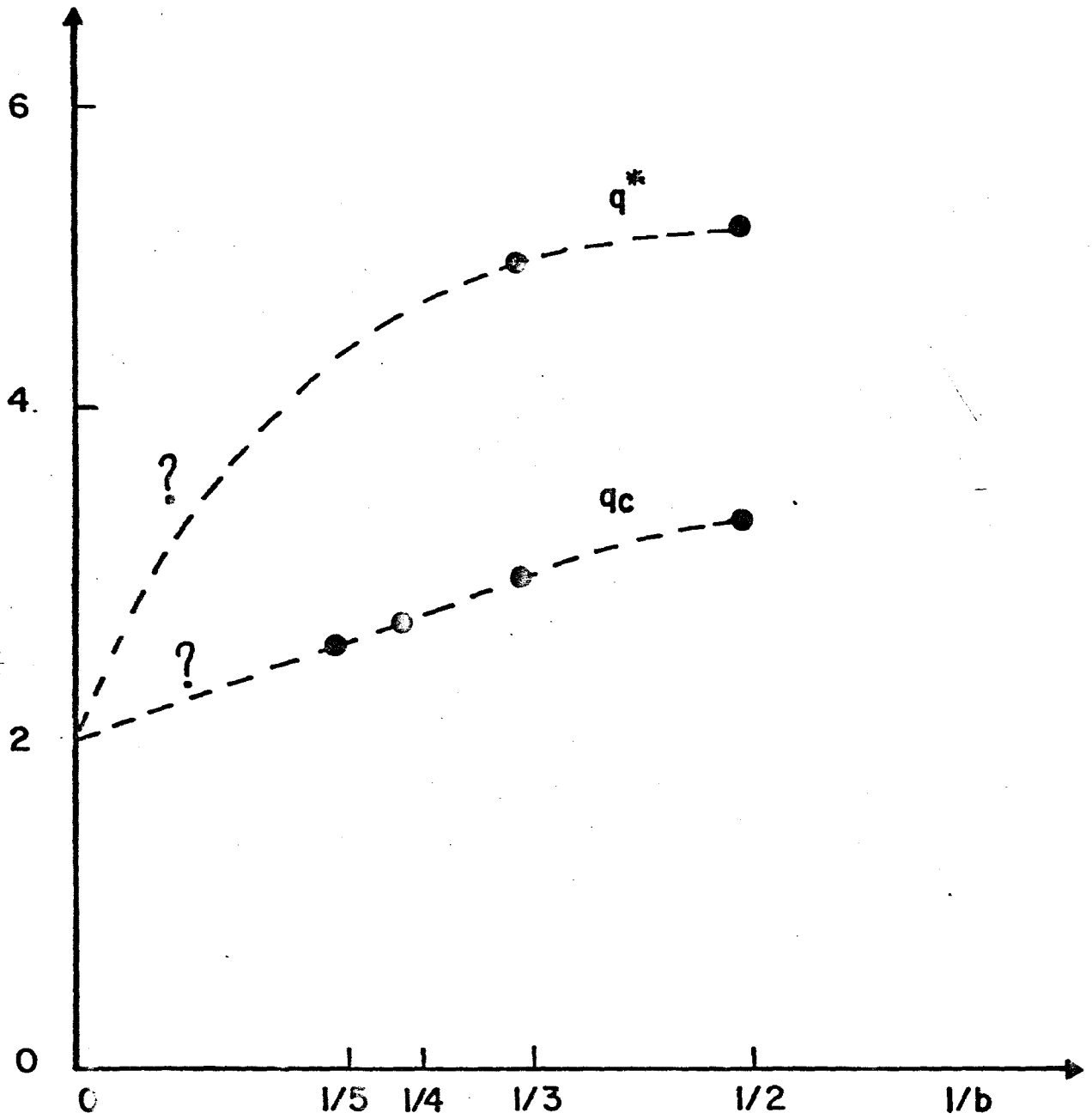


FIG. 8

TABLE I

ℓ	m_ℓ	M_ℓ	t_ℓ
1	0	1	$\frac{2t_2^2+2t_2^3+5(q-2)t_2^4+(q-2)(q-3)t_2^5}{1+(q-1)(2t_2^3+t_2^4)+(q-1)(q-2)t_2^5}$
2	1	1	$\frac{2t_2^2+2t_2^2t_1+(q-2)(t_2^4+4t_2^3t_1)+(q-2)(q-3)t_1t_2^4}{1+(q-1)(t_2^4+2t_2^2t_1)+(q-1)(q-2)t_2^4t_1}$
3	1	4	$\frac{t_2t_1+t_2^2+t_2^2t_1+t_2^3+(q-2)(4t_2^3t_1+t_2^4)+(q-2)(q-3)t_2^4t_1}{1+(q-1)(t_2^2t_1+t_2^3+t_2^3t_1)+(q-1)(q-2)t_2^4t_1}$
4	2	2	$\frac{2t_2t_1+2t_2^2t_1+(q-2)(3t_2^2t_1^2+2t_2^3t_1)+(q-2)(q-3)t_2^3t_1^2}{1+(q-1)(t_2t_1^2+t_2^2t_1^2+t_2^3)+(q-1)(q-2)t_2^3t_1^2}$
5	2	2	$\frac{2t_2t_1+t_2t_1^2+t_2^3+(q-2)(3t_2^2t_1^2+2t_2^3t_1)+(q-2)(q-3)t_2^3t_1^2}{1+(q-1)(2t_2^2t_1+t_2^2t_1^2)+(q-1)(q-2)t_2^3t_1^2}$
6	2	2	$\frac{t_2^2+2t_2^2t_1+t_1^2+(q-2)(3t_2^2t_1^2+2t_2^3t_1)+(q-2)(q-3)t_2^3t_1^2}{1+(q-1)(2t_2^2t_1+t_2^2t_1^2)+(q-1)(q-2)t_2^3t_1^2}$
7	2	4	$\frac{t_2t_1+t_2^2+t_2^2t_1+t_2t_1^2+(q-2)(3t_2^2t_1^2+2t_2^3t_1)+(q-2)(q-3)t_2^3t_1^2}{1+(q-1)(t_2t_1^2+t_2^2t_1+t_2^3t_1)+(q-1)(q-2)t_2^3t_1^2}$
8	3	4	$\frac{t_1t_2+t_1^2+t_1^2t_2+t_1t_2^2+(q-2)(3t_1^2t_2^2+2t_1^3t_2)+(q-2)(q-3)t_1^3t_2^2}{1+(q-1)(t_1t_2^2+t_1^2t_2+t_1^3t_2)+(q-1)(q-2)t_1^3t_2^2}$
9	3	2	$\frac{t_1^2+2t_1^2t_2+t_2^2+(q-2)(3t_1^2t_2^2+2t_1^3t_2)+(q-2)(q-3)t_1^3t_2^2}{1+(q-1)(2t_1^2t_2+t_1^2t_2^2)+(q-1)(q-2)t_1^3t_2^2}$
10	3	2	$\frac{2t_1t_2+t_1t_2^2+t_1^3+(q-2)(3t_1^2t_2^2+2t_1^3t_2)+(q-2)(q-3)t_1^3t_2^2}{1+(q-1)(2t_1^2t_2+t_1^2t_2^2)+(q-1)(q-2)t_1^3t_2^2}$
11	3	2	$\frac{2t_1t_2+2t_1^2t_2+(q-2)(3t_1^2t_2^2+2t_1^3t_2)+(q-2)(q-3)t_1^3t_2^2}{1+(q-1)(t_1t_2^2+t_1^2t_2^2+t_1^3)+(q-1)(q-2)t_1^3t_2^2}$
12	4	4	$\frac{t_1t_2+t_1^2+t_1^2t_2+t_1^3+(q-2)(4t_1^3t_2+t_1^4)+(q-2)(q-3)t_1^4t_2}{1+(q-1)(t_1^2t_2+t_1^3+t_1^3t_2)+(q-1)(q-2)t_1^4t_2}$
13	4	1	$\frac{2t_1^2+2t_1^2t_2+(q-2)(t_1^4+4t_1^3t_2)+(q-2)(q-3)t_2t_1^4}{1+(q-1)(t_1^4+2t_1^2t_2)+(q-1)(q-2)t_1^4t_2}$
14	5	1	$\frac{2t_1^2+2t_1^3+5(q-2)t_1^4+(q-2)(q-3)t_1^5}{1+(q-1)(2t_1^3+t_1^4)+(q-1)(q-2)t_1^5}$

TABLE II

$b \backslash q$	1	2	3	4
2	1.4277	1.1486	1.0236	0.9484
3	1.3797	1.1094	0.9883	0.9156
4	1.3627	1.0950	0.9752	0.9033
5	1.3553	1.0879	0.9684	0.8966
Exact	$4/3$	1	$5/6$	$2/3$

TABLE III

q	$-\frac{ds_2}{dp} \Big _{\substack{s_1=0 \\ p_2=1}}$	$\frac{1}{T_c(1)} \frac{dT_c(p)}{dp} \Big _{p=1}$	error (see Eq. (7))
1	1/2	1.443	0%
2	0.495	1.329	0.1%
3	0.490	1.267	0.4%
4	0.488	1.232	1.5%

TABLE V

$\frac{J_1}{J_2} \frac{k_1^T/q_1^2}{q_2}$	0.2	0.4	0.6	0.8	1.0	1.2	1.4	1.6	1.8	2.0	2.2	2.4	2.6	2.8	3.0	3.2	3.4	3.6	
0	1	0.5034	0.5447	0.6164	0.7008	0.7910	0.8843	0.9795	-	-	-	-	-	-	-	-	-	-	-
	2	0.5000	0.5049	0.5265	0.5640	0.6116	0.6656	0.7237	0.7845	0.8473	0.9116	0.9771	-	-	-	-	-	-	-
	3	0.5000	0.5005	0.5061	0.5217	0.5469	0.5796	0.6176	0.6594	0.7040	0.7507	0.7990	0.8487	0.8995	0.9513	-	-	-	-
	4	0.5000	0.5000	0.5013	0.5072	0.5199	0.5391	0.5640	0.5932	0.6257	0.6607	0.6977	0.7363	0.7762	0.8173	0.8593	0.9022	0.9461	0.9907
0.05	1	0.3611	0.4779	0.5745	0.6730	0.7735	0.8753	0.9780	-	-	-	-	-	-	-	-	-	-	-
	2	0.2699	0.4033	0.4614	0.5165	0.5752	0.6374	0.7020	0.7686	0.8365	0.9056	0.9756	-	-	-	-	-	-	-
	3	0.1764	0.3666	0.4217	0.4601	0.4986	0.5403	0.5852	0.6326	0.6820	0.7330	0.7853	0.8386	0.8930	0.9482	-	-	-	-
	4	0.0701	0.3337	0.3985	0.4327	0.4614	0.4912	0.5237	0.5588	0.5962	0.6354	0.6762	0.7183	0.7614	0.8055	0.8505	0.8963	0.9429	0.9902
0.5	1	-	-	-	0.1418	0.4464	0.7089	0.9502	-	-	-	-	-	-	-	-	-	-	-
	2	-	-	-	-	-	0.0766	0.2828	0.4646	0.6328	0.7927	0.9473	-	-	-	-	-	-	-
	3	-	-	-	-	-	-	-	0.0942	0.2504	0.3914	0.5232	0.6491	0.7713	0.8909	-	-	-	
	4	-	-	-	-	-	-	-	-	0.1264	0.2519	0.3673	0.4764	0.5813	0.6832	0.7841	0.8828	0.9802	